Mineral Processing & Extractive Metall. Rev., 35: 239–256, 2014

ISSN: 0882-7508 print/1547-7401 online
DOI: 10.1080/08827508.2013.766793

KINETIC ANALYSIS OF ISOTHERMAL DECOMPOSITION PROCESS OF ZINC LEACH RESIDUE IN AN INERT ATMOSPHERE. THE ESTIMATION OF THE APPARENT ACTIVATION ENERGY DISTRIBUTION

Bojan Janković[1], Srećko Stopić[2], Aybars Güven[2], and Bernd Friedrich[2]
[1]*Department for Dynamics and Matter Structure, Faculty of Physical Chemistry, University of Belgrade, Belgrade, Serbia*
[2]*IME Process Metallurgy and Metal Recycling, RWTH Aachen University, Aachen, Germany*

Thermal decomposition of zinc leach residue has been studied in a tubular furnace under a constant nitrogen gas flowing, at four different operating temperatures (600°C, 750°C, 950°C, and 1150°C). Using a detailed kinetic analysis, it was shown that the investigated process can be described by a two-parameter autocatalytic Šesták–Berggren reaction model. It was noted that the apparent activation energy values E_a increase progressively with a degree of conversion, accompanied by the appearance of a convex Arrhenius dependence. This behavior is a characteristic of a system of parallel competing reactions. It was concluded that the investigated isothermal decomposition process is characterized by unusually very low preexponential factor and low values of the apparent activation energy. Based on the derived density distribution function of E_a values, it was concluded that the isothermal decomposition process probably occurs through four reaction steps, where each step is characterized by one parallel reaction.

Keywords: agglomeration, furnaces, hydrothermal processing, mathematical modeling, reduction, zinc

INTRODUCTION

Because zinc leach residue is of great interest for environmental protection in metallurgical industry, the study of thermal decomposition is required. Decomposition of Zn–ferrite for O_2 generation by the concentrated solar radiation was performed in two steps (Kaneko et al. 2004). The reduction plots of zinc ferrite solid solutions exhibited an initial linear rate followed by a gradual decrease in rate with increased percentage reduction. Two possible reactions for decomposition of Zn–ferrite were proposed (Kaneko et al. 2004):

$$3ZnFe_2O_4 \rightarrow 3Zn + 2Fe_3O_4 + 2O_2 \qquad (1)$$

Address correspondence to Bojan Janković, Department for Dynamics and Matter Structure, Faculty of Physical Chemistry, University of Belgrade, Studentski Trg 12-16, Belgrade, Serbia. E-mail: bojanjan@ffh.bg.ac.rs

$$6ZnFe_2O_4 \rightarrow 6ZnO + 4Fe_3O_4 + O_2 \tag{2}$$

It was finally concluded that the Zn–ferrite decomposition reaction by the irradiation of the concentrated beam mainly proceeds with the release of O_2 according to Equation (1). The solar decomposition of Zn–ferrite can be promoted with an increased temperature above 1477°C.

A part of zinc is also recovered from different secondary resources, such as leach residue, zinc ash and dross, electric arc furnace dust, automobile shredder scrap, and rayon industry sludge, which contain different levels of impurities depending on their sources. Solid residue after neutral leaching (SRANL) in zinc electrowinning is one of the most important secondary materials for metal recovery. The toxicity is mainly due to the presence of metals, such as lead, cadmium, arsenic, and chromium (Radović, Amberović, and Panias 2009). Given the high toxicity of lead, the current efforts try to eliminate the use of lead in all applications wherever possible. A kinetic study of hydrometallurgical and pyrometallurgical processes employed for the recovery of zinc and removal of lead from a zinc plant residue was reported (Štrbac et al. 2011). The maximum zinc recovery obtained during a pyrometallurgical treatment was 72% at 1300°C.

Leaching with dilute sulfuric acid to obtain high recovery yield proved feasible based on the following reaction:

$$ZnFe_2O_4 + 4H_2SO_{4\,(aq)} \rightarrow ZnSO_{4\,(aq)} + Fe_2(SO_4)_3 + 4H_2O. \tag{3}$$

The dissolution presented by Equation (3) at a low rate can be observed even at ambient temperatures.

During this process, calcium sulfate precipitates resulting from the low concentration of sulfuric acid and it remains until the end of the process. Because of unselective leaching, the yield of zinc is decreased (Havlik et al. 2007):

$$ZnFe_2O_4{+}2[OH^-] \rightarrow ZnO_2^{2-} + Fe_2O_3 + H_2O. \tag{4}$$

Hydrochloric acid can also be used for zinc extraction from electric arc furnace (EAF) dust according to the leaching reaction in Equation (5):

$$ZnFe_2O_4 + 2HCl \rightarrow ZnCl_2 + Fe_2O_3 + H_2O. \tag{5}$$

A new concept was developed for the thermal decomposition of zinc ferrite (Stopić and Friedrich 2009). The aim was to release zinc oxide from zinc ferrite in the leach residue and in zinc containing flue dust. The phase analysis of the untreated as well as the thermally treated material confirmed the presence of ZnO and Fe_3O_4 after decomposition, and zinc can be recovered thus avoiding reduction and evaporation. The test was performed only at 1150°C in a tube furnace in a nitrogen atmosphere.

This study presents a detailed kinetic analysis of the isothermal decomposition process of zinc leach residue in an inert atmosphere between 600°C and 1150°C and investigates the corresponding distribution of the apparent activation energies (Burnham and Braun 1999).

EXPERIMENTAL

Characterization Methodology

The zinc leach residue was obtained from former company Ruhr-Zink, Datteln, Germany with a moisture content of 23%. Before the experimental investigation, the sample was dried at 120°C overnight in order to eliminate the moisture. Rietveld X-ray diffraction (XRD) analysis of an initial sample has shown the following chemical composition (in %): 40.9 $ZnFe_2O_4$, 16.5 $CaSO_4$, 6.4 $MgSO_4$, 13.6 Zn_2SiO_4, 11.3 $PbSO_4$, 4.4 $KFe_3(SO_4)_2(OH)_6$, and 6.9 related to the other compounds. This phase change made materials more soluble and suitable for the leaching process, which was previously reported (Stopić and Friedrich 2009). The gaseous phases of PbO and SO_2 were formed during thermal decomposition and removed with nitrogen as carrier gas. At 1150°C, the chemical composition of the final decomposed material amounted to (in %): 57.0 Fe_3O_4, 28.9 $Ca_2ZnSi_2O_7$, 8.4 ZnO, 5.0 Mg_2SiO_6, and 0.7 $ZnAl_2O_4$.

Isothermal Measurements in an Inert Atmosphere

After 15 min of heating the samples in order to eliminate the contained moisture, these were used in the thermal treatment experiments performed in the tube furnace. At the fixed operating temperatures (600, 750, 900, and 1150°C), the four experiments were performed at each temperature in certain time intervals (15, 20, 25, 30, 35, 40, 45, 50, 55, and 60 min). The experiments were repeated three times. After reaching the aimed temperature, 1 g of the zinc leach residue was inserted in a tubular furnace, under a constant nitrogen gas, with a flow rate of $\varphi = 1\,\mathrm{L\,min^{-1}}$. After beginning of the thermal treatment of dried sample at the fixed operating temperature, the reaction time was measured by a chronometer (in digits form). After that, the specimen was taken out from the furnace and placed in the exsiccator. The weight results were noted as an average mass lost by the specimen, in order to calculate the decomposition rate.

The conversion fraction (α) in the isothermal measurement at considered operating temperature T is calculated by the following equation:

$$\alpha = \frac{m_{o(15)} - m_t}{m_{o(15)} - m_f}, \tag{6}$$

where $m_{o(15)}$ is the initial mass of the sample (for $t = 15$ min, after removing any remaining moisture at a given temperature (the time period from $t = 0$ min to $t = 15$ min at each considered temperature T corresponds to time scale where the removal was done for possible residual moisture)), m_t is the mass of the sample at time t, and m_f is the final constant mass of the sample, after the establishment of saturation (saturation involves reaching the conversion value of $\alpha = 1$). Thus, the conversion data are calculated for completely dry samples at each of the observed temperatures. The decomposition of zinc leach residue in an inert atmosphere at every considered operating temperature begins after the 15th minute.

KINETIC ANALYSIS

The rate of a solid state decomposition process can be generally described by

$$\frac{d\alpha}{dt} = kf(\alpha), \tag{7}$$

where k is the rate constant, $f(\alpha)$ is the differential reaction model, and α is the conversion fraction or the extent of reaction. Integrating this equation gives the integral rate law of the form (Galwey and Brown 1999):

$$g(\alpha) = kt \qquad (8),$$

where $g(\alpha)$ is the integral reaction model. The temperature dependence of the rate constant is usually described by the Arrhenius equation:

$$k = A\exp\left(-\frac{E_a}{RT}\right), \tag{9}$$

where A is the preexponential (frequency) factor, E_a is the apparent activation energy, T is the absolute temperature, and R is the gas constant. Substituting Equation (9) in the previous two rate expressions gives

$$\frac{d\alpha}{dt} = A\exp\left(-\frac{E_a}{RT}\right)f(\alpha) \tag{10}$$

and

$$g(\alpha) = A\exp\left(-\frac{E_a}{RT}\right)t. \tag{11}$$

For the different solid state reaction mechanisms, $f(\alpha)$ and $g(\alpha)$ have different expressions (Turmanova et al. 2008). The most frequently cited kinetic models used in this article are given by Turmanova et al. (2008).

Kinetic parameters can be obtained from isothermal kinetic data by applying these rate laws with traditional model-fitting methods or with isoconversional (model-free) methods. Model-fitting methods involve two fits: the first determines the model that best fits the data (Equation (8)), while the second determines specific kinetic parameters such as the apparent activation energy (E_a) and the preexponential factor (A) using the Arrhenius equation.

On the other hand, isoconversional methods calculate E_a values at progressive degrees of conversions without any modelistic assumptions. The standard isoconversional method (Vyazovkin 2000) is based on taking the natural logarithm of Equation (11) giving,

$$-\ln(t_{\alpha,i}) = \ln\left[\frac{A_\alpha}{g(\alpha)}\right] - \frac{E_{a,\alpha}}{RT_i}, \tag{12}$$

where $t_{\alpha,\ i}$ is the time at a given value of α for operating temperature T_i, while A_α represents the preexponential factor at a given value of conversion. From different isothermal runs for which same values of α were reached, linear plots $-\ln(t_{\alpha,\,i})$ versus $1/T_i$ with slope proportional to E_a can be drawn. This method may give a model-independent value of the apparent activation energy.

Friedman's (1964) method is based on taking the natural logarithm of Equation (10) giving

$$\ln\left(\frac{\mathrm{d}\alpha}{\mathrm{d}t}\right)_{\alpha,i} = \ln[A_\alpha f(\alpha)] - \frac{E_{a,\alpha}}{RT_i}, \tag{13}$$

where $(d\alpha/dt)_{\alpha,i}$ represents the rate of process at a given value of α for the operating temperature T_i. A plot of $\ln(\mathrm{d}\alpha/\mathrm{d}t)_{\alpha,i}$ versus $1/T_i$ at each α yields E_a (from the slope of the straight line).

Since at a constant temperature, $k = g(\alpha)/g(0.50)$, a relationship between $t_{0.50}$ and temperature is written as (Bamford and Tipper 1980)

$$\ln\left(\frac{1}{t_{0.50}}\right) = \ln(A) - \ln[g(0.50)] - \left(\frac{E_a}{R}\right)\frac{1}{T}. \tag{14}$$

For each isothermal run, the values of time (t) to reach $\alpha = 0.50$ were calculated. The slope of the linear curve provides the value of E_a. It is important to notice that the induction time (the time between the beginning of the experiment and the actual beginning of the reaction) must be brought down to $t_{0.50}$.

In addition to determining the apparent activation energy, it is desirable to find an appropriate reaction model that best describes the kinetics of the investigated process. A kinetic method for determining the most accurate function $f(\alpha)$ or $g(\alpha)$ was proposed by Málek (1992).

Combining Equations (10) and (11), a new function $Z(\alpha)$ can be obtained (Málek 1992):

$$Z(\alpha) = \left(\frac{\mathrm{d}\alpha}{\mathrm{d}t}\right)t = f(\alpha)g(\alpha). \tag{15}$$

For practical reasons, this function is normalized within the (0,1) interval. It was shown (Málek and Smrčka 1991) that the maximum of $Z(\alpha)$ function (designated by $\alpha_p{}^{\infty}$) has characteristic values for basic reaction models. The function $Z(\alpha)$ is useful for the classification of possible reaction model, $f(\alpha)$. In isothermal conditions, however, the term $A\cdot\exp(-E_a/RT)$ in Equation (10) is constant and the rate $(\mathrm{d}\alpha/\mathrm{d}t)$ is proportional to the $f(\alpha)$ function as

$$Y(\alpha) = \left(\frac{\mathrm{d}\alpha}{\mathrm{d}t}\right) \approx f(\alpha). \tag{16}$$

Therefore, if the reaction rate is plotted as a function of α, its shape corresponds to the $f(\alpha)$ function. It is convenient to normalize the $Y(\alpha)$ plot within the (0,1) interval. The shape of this plot (with the maximum designated by α_m) is a characteristic for each kinetic model and it can be used as the diagnostic tool for the determination of the kinetic model (Málek 1992).

RESULTS AND DISCUSSION

The experimentally obtained isothermal conversion ($\alpha - t$) curves for the decomposition process of the dry zinc leach residue samples, at the operating temperatures of 600°C, 750°C, 950°C, and 1150°C in an inert atmosphere, are presented in Figure 1.

The rate of decomposition increases with an increase in operating temperature, and at $T = 1150°\text{C}$, approximately 100% is achieved in less than 35 min. In that case, the isothermal decomposition of zinc leach residue in an inert atmosphere should be performed at operating temperatures $T \geq 600°\text{C}$ to investigate the whole decomposition process within a reasonable time period.

The experimental differential conversion ($d\alpha/dt - t$) curves obtained at the different operating temperatures (600°C, 750°C, 950°C, and 1150°C) for the decomposition process of zinc leach residue are shown in Figure 2. The differential conversion curves in Figure 2 were presented in the *B*-spline graphics mode. The curves are obtained by numerical differentiation of the conversion (integral) $\alpha - t$ curves (Figure 1).

Figure 2 shows that all $\mathrm{d}\alpha/\mathrm{d}t$ versus t curves exhibit the maximum decomposition rate ($(\mathrm{d}\alpha/\mathrm{d}t)_{\mathrm{max}}$) at value $t_{\mathrm{max}} > 0$. The increase in operating temperature leads to a narrowing of the reaction profiles on the considered differential conversion curves (Figure 2). Table 1 shows the values of $(\mathrm{d}\alpha/\mathrm{d}t)_{\mathrm{max}}$, $(\mathrm{d}\alpha/\mathrm{d}t)_{\mathrm{max}}/2$ (the rate corresponding to half the maximum value), $t_{m/2}{}^{*}$ (the time on the descent of the corresponding $\mathrm{d}\alpha/\mathrm{d}t$ versus t curve), and t_{max} (the time that corresponds to a value of $(\mathrm{d}\alpha/\mathrm{d}t)_{\mathrm{max}}$) for differential conversion ($\mathrm{d}\alpha/\mathrm{d}t$ versus t) curves in Figure 2.

It can be seen from Table 1 that the values of $(\mathrm{d}\alpha/\mathrm{d}t)_{\mathrm{max}}$ and $(\underline{\mathrm{d}}\alpha/\mathrm{d}t)_{\mathrm{max}}/2$ increase with an increasing operating temperature, while the values of $t_{m/2}{}^{*}$ and t_{max} decrease with an increasing temperature from 600°C to 1150°C, which directly indicates the narrowing of the reaction profile.

The presented rate–time features of differential conversion curves are useful for the basic classification of kinetic models. Thus, the above results are designated on the sigmoid group of kinetic (nucleation) models, such as JMA (Johnson–Mehl–Avrami),

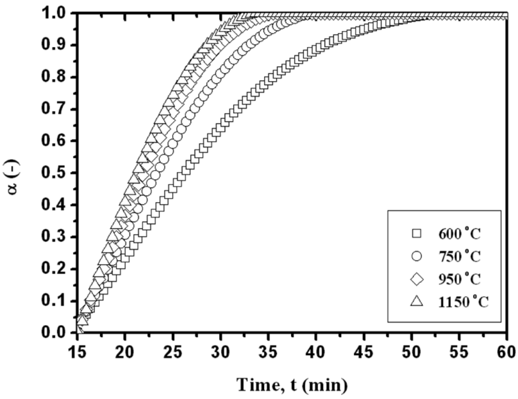

Figure 1. Experimentally obtained conversion curves for investigated isothermal decomposition process, at the different operating temperatures (600°C, 750°C, 950°C, and 1150°C) in an inert atmosphere.

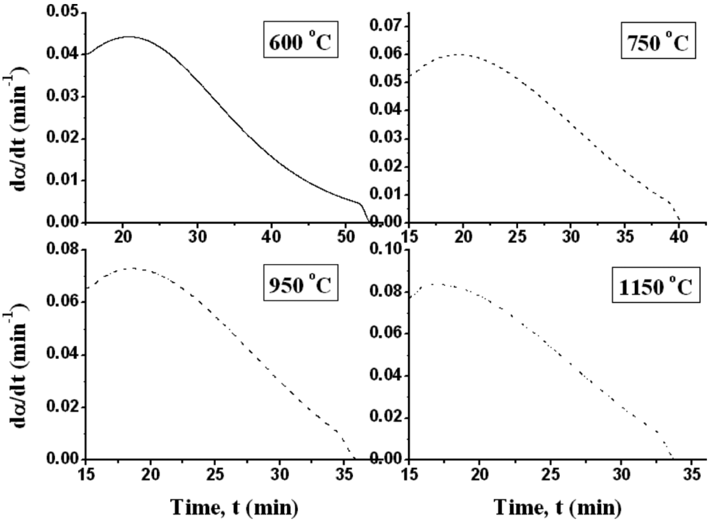

Figure 2. The differential conversion curves obtained at the different operating temperatures (600°C, 750°C, 950°C, and 1150°C), for the isothermal decomposition process of zinc leach residue in an inert atmosphere. All $d\alpha/dt - t$ curves are presented in the *B*-spline graphics mode.

SB (Šesták–Berggren), or PT (Prout–Tompkins) (this group has $(d\alpha/dt) = (d\alpha/dt)_{max}$ at $t = t_{max} > 0$) (Brown and Galwey 1989). Furthermore, as shown in Figure 2, the decomposition rate peak becomes higher and shifts to the shorter times when the operating temperature increases. This behavior confirms the existence of an autocatalytic mechanism (which results in a bell-shaped reaction rate versus time curve) for the investigated decomposition process. However, the aforementioned discussion is only a preliminary analysis of the reaction mechanism, which could adequately describe the observed process.

Figure 3 shows the dependence of the decomposition rates ($d\alpha/dt$) on the conversion (α) for the decomposition process of zinc leach residue, at different operating temperatures.

Obviously, increasing the operating temperatures leads to systematically increased $d\alpha/dt$, that is, $d\alpha/dt$ is a positive function of the operating temperature at same α. However, maximum $d\alpha/dt$ appears at the different values of α_{max} (Figure 3), which vary in the conversion range of $0.150 \leq \alpha_{max} \leq 0.281$ and indicate

Table 1. The rate–time features $(d\alpha/dt)_{max}$, $(d\alpha/dt)_{max}/2$, $t_{m/2}^*$, and t_{max} for differential conversion curves of the isothermal zinc leach residue decomposition process, at the different operating temperatures (600°C, 750°C, 950°C, and 1150°C)

Temperature, *T* (°C)	$(d\alpha/dt)_{max}$ (min^{-1})	$(d\alpha/dt)_{max}/2$ (min^{-1})	$t_{m/2}^*$ (min)	t_{max} (min)
600	0.04433	0.02217	36.595	20.909
750	0.06019	0.03009	31.470	19.545
950	0.07307	0.03654	28.683	18.636
1150	0.08371	0.04186	27.167	16.818

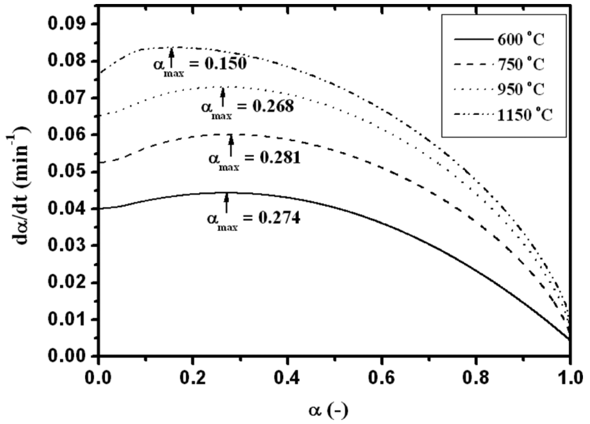

Figure 3. The reaction rate $d\alpha/dt$ as a function of conversion α at the different operating temperatures (600°C, 750°C, 950°C, and 1150°C), for the isothermal decomposition process of zinc leach residue (maximum positions $\alpha_{\max}$ of the given reaction rate curves are marked on the same figure).

the dependence on the operating temperature. This behavior implies that the fundamental reaction mechanism may change.

Knowing $d\alpha/dt$ and product $(d\alpha/dt)\cdot t$ allows us to make a selection of the kinetic model that best describes the investigated process, according to the Málek (1992) method. The substitution of $d\alpha/dt$ and t values into Equations (16) and (15) give normalized $Y(\alpha)$ and $Z(\alpha)$ functions (Origin 8.5® Software was used for calculation), as shown in Figures 4 and 5.

From Figures 4 and 5, we can see that the $Y(\alpha)$ and $Z(\alpha)$ functions vary with operating temperature, which indicates the complex decomposition mechanism. On the basis of such behavior of the $Y(\alpha)$ and $Z(\alpha)$ functions, it is reasonable to assume that the characteristic conversion values or maxima of a given function (α_m for $Y(\alpha)$ function and α_p^{∞} for $Z(\alpha)$ function) will also vary with operating temperature, as in the case of $\alpha_{\max}$ values.

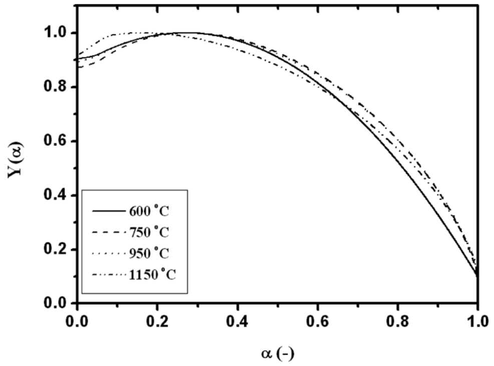

Figure 4. Plots of normalized $Y(\alpha)$ against α at the different operating temperatures (600°C, 750°C, 950°C, and 1150°C), for the isothermal decomposition process of zinc leach residue.

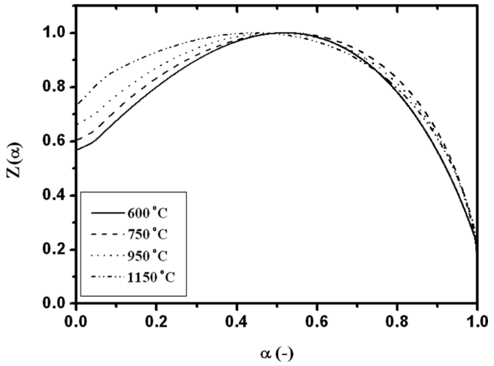

Figure 5. Plots of normalized $Z(\alpha)$ against α at the different operating temperatures (600°C, 750°C, 950°C, and 1150°C), for the isothermal decomposition process of zinc leach residue.

Table 2 shows the values of α_m and α_p^∞ for the calculated $Y(\alpha)$ and $Z(\alpha)$ functions, which vary with operating temperature, within the following conversion ranges: $0.150 \le \alpha_m \le 0.281$ and $0.445 \le \alpha_p^\infty \le 0.526$, respectively.

These values fulfill conditions $\alpha_p^\infty \neq 0.623$ and $\alpha_m \in (0, \alpha_{\max})$ for the same operating temperature. According to the criteria proposed by Málek (1992), this confirms that the two-parameter autocatalytic SB kinetic model (Šesták and Berggren 1971) should be used to describe the isothermal reaction rate of zinc leach residue decomposition:

$$\frac{d\alpha}{dt} = A \exp\left(-\frac{E_a}{RT}\right)\alpha^m(1-\alpha)^n, \tag{17}$$

where m and n are the reaction orders (or SB kinetic exponents); m being an independent reaction order. If the geometric–probabilistic interpretation is used, it should be taken into account that any choice of $m \neq 1$ negates the fundamental assumption of the equiprobability of the nuclei formation.

If the testing kinetic method reveals that the Johnson–Mehl–Avrami model cannot be applied, for instance, if there is a considerable overlap in the nucleation and growth processes, then the two parametric SB empirical equations can be used

Table 2. The maximum values of $Y(\alpha)$ and $Z(\alpha)$ functions (α_m and α_p^∞ values, respectively) for the isothermal decomposition process of zinc leach residue, at the different operating temperatures ($T = 600$°C, 750°C, 950°C, and 1150°C)

Temperature, T (°C)	α_m	α_p^∞
600	0.274	0.526
750	0.281	0.520
950	0.268	0.495
1150	0.150	0.445
Average	0.243	0.497

for a quantitative description of the overall isothermal decomposition. The value of exponent m in Equation (17) should be confined to the range of $0 < m < 1$.

In Equation (17), the ratio of reaction order m to n, $p = m/n$, as pointed out by Málek (1992) can be replaced by

$$p = \frac{\alpha_m}{(1 - \alpha_m)}, \tag{18}$$

where α_m is the conversion for the peak value of $Y(\alpha)$ function.

In addition, the logarithmic transformation and rearrangements of Equations (17) and (18) yield:

$$\ln\left[\left(\frac{\mathrm{d}\alpha}{\mathrm{d}t}\right) \cdot \exp\left(\frac{E_a}{RT}\right)\right] = \ln A + n \ln[\alpha^p(1 - \alpha)]. \tag{19}$$

Equation (19) can be used to determine the reaction order n and the preexponential factor A from the slope and the intercept of the linear plot of $\ln[(\mathrm{d}\alpha/\mathrm{d}t) \cdot \exp(E_a/RT)]$ versus $\ln[\alpha^p(1 - \alpha)]$ for $\alpha \in [0.20, 0.80]$, respectively. The reactions that take place in the solid state usually occur in the initial phase of the investigated process. This phenomenon is almost inevitable even under the strict control of the sample size. As a result, the values of the apparent activation energy at the beginning (for $\alpha = 0.10$ or $\alpha = 0.15$) and at the end (for $\alpha = 0.85$ or $\alpha = 0.90$) may differ from the values of E_a in the middle part of the considered process (for $\alpha = 0.50$). In this way, using the values of the apparent activation energies that were calculated for the initial and final stages of the investigated process can lead to large errors (Roşu et al. 2002). Thus, the extreme conversion ranges should be excluded in the calculation of the kinetic parameters.

The apparent activation energy based on Equation (14) was $E_a = 4.0 \pm 0.2$ kJ mol^{-1}. This value of E_a is inserted into Equation (19), in order to calculate the parameter n at the different operating temperatures. The effect of the operating temperature on the kinetic exponents (m and n) and the preexponential factor (A) for the decomposition process of the zinc leach residue is presented in Table 3.

Table 3. The estimated kinetic exponents m and n and the preexponential factor A, for the decomposition process of zinc leach residue at the different operating temperatures, using the Šesták–Berggren (SB) kinetic model. The values of α_{max} are also given in the same table

Temperature, T (°C)	m	n	$m + n$[a]	A (min^{-1})	α_{max}	R^2[b]	RSS[c]
600	0.275 ± 0.003	0.729 ± 0.003	1.004	0.1397	0.274	0.99932	9.594×10^{-4}
750	0.226 ± 0.002	0.577 ± 0.001	0.803	0.1555	0.281	0.99989	6.079×10^{-5}
950	0.206 ± 0.003	0.562 ± 0.002	0.768	0.1696	0.268	0.99986	6.005×10^{-5}
1150	0.087 ± 0.006	0.495 ± 0.005	0.582	0.1533	0.150	0.99786	1.070×10^{-3}
Average	0.199 ± 0.004	0.591 ± 0.003	0.789	0.1545	0.243	–	–

[a] The global reaction order.

[b] Adj. R-square.

[c] Residual sum of squares (RSS).

The values of m are smaller than those of n, and $m+n$ (the global reaction order) is approximately within the range of 0.500–1.000. Moreover, the values of parameters m and n lay within the range of $0.087 \leq m \leq 0.275$ and $0.495 \leq n \leq 0.729$, respectively. The parameter m reaches a very low value at the highest operating temperature of $T = 1150°\mathrm{C}$. The fact that the value of m is lower than unity means that the autocatalytic reaction has higher contribution on the overall reaction rate. For $m \neq 0$ and $n \neq 0$, the SB reaction model function, $f(\alpha)$, reaches a maximum for a value of α ($\alpha_{\max}$) that depends on both m and n (Málek and Smrčka 1991):

$$\alpha_{\max} = \frac{m}{m+n}. \tag{20}$$

The values of $\alpha_{\max}$ at every considered operating temperature are also presented in Table 3. It can be seen that when the $m+n$ values become close to each other, the values of $\alpha_{\max}$ also follow the same trend. This is typical for lower operating temperatures, such as 600°C and 750°C.

At the operating temperatures above 950°C, the autocatalytic effect becomes more noticeable. On the other hand, low values of the preexponential factors (A) may indicate a surface reaction, but if the reactions are not dependent on the surface area, the low preexponential factor can also point to a "tight" complex. In our case, most likely when increasing the operating temperature, the enthalpy effect to the reaction rate becomes flattered and the tendency to association (to create complex), represented by the preexponential factor, gets more important, thus the autocatalyzed decomposition becomes more important at the higher operating temperatures (Turmanova et al. 2008).

Substitution of the average values of calculated parameters from Table 3 into the SB kinetic model produces the explicit rate equation (Equation (21)) based on autocatalyzed kinetics in Equation (17):

$$\frac{\mathrm{d}\alpha}{\mathrm{d}t} = 0.1545 \cdot \exp\left(-\frac{4000}{RT}\right) \cdot \alpha^{0.199}(1-\alpha)^{0.591}. \tag{21}$$

The accuracy of the obtained n values in Table 3 can be checked by the model for autocatalyzed kinetics in Equation (17). Taking into account the value of the global reaction order $m+n$, Equation (17) can be rearranged and expressed as

$$\ln\left[\frac{\left(\frac{\mathrm{d}\alpha}{dt}\right)}{\alpha^{m+n}}\right] = \ln k + n \ln\left[\frac{(1-\alpha)}{\alpha}\right]. \tag{22}$$

This form can now be used to determine k and n (from the intercept and the slope of the linear expression, respectively). The linear regressions were performed at the different operating temperatures and for the global reaction orders from Table 3 (Figure 6a–d).

Very high values of the Adj. R-Square (R^2) were achieved for all considered global reaction orders and for all operating temperatures. Only the linear portion of the data was fit to a linear regression to determine rate constants (k) and reaction

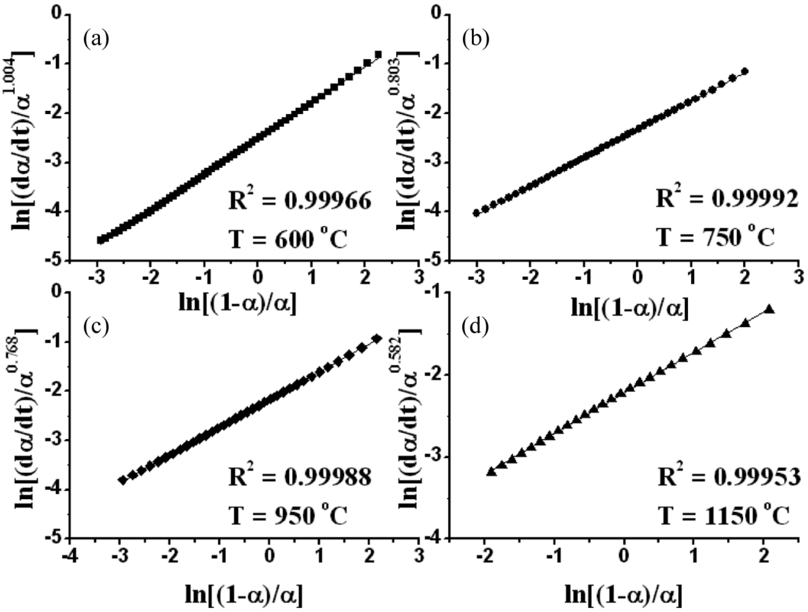

Figure 6. The dependence of $\ln[(d\alpha/dt)/\alpha^{m+n}]$ versus $\ln[(1-\alpha)/\alpha]$, for the isothermal decomposition process of zinc leach residue, at the different operating temperatures ((a) 600°C, (b) 750°C, (c) 950°C, and (d) 1150°C) (R^2 is the Adj. R-square).

orders (n). Table 4 lists the values of rate constants and reaction orders calculated using Equation (22), at the different operating temperatures.

There is an excellent agreement between the n values predicted by using Equation (22) and n values calculated on the basis of experimental results (Tables 3 and 4).

Based on the aforesaid results, we can *assume* that the investigated zinc leach residue decomposition occurs as a complex process, which probably involves the various elementary reaction pathways. Consequently, using a single reaction rate equation to accurately untangle this complexity often yields very vague results (Vyazovkin and Wight 1999) because it is practically impossible to take all kinetic complexities into account with a single rate equation. However, the fundamental

Table 4. The values of the rate constants (k) and reaction orders (n) calculated using Equation (22), at the different operating temperatures, for decomposition process of zinc leach residue

Temperature, T (°C)	k (min^{-1})	n
600	0.08090	0.730
750	0.09739	0.577
950	0.10868	0.563
1150	0.11476	0.495

assumption of the isothermal isoconversional methods is that a single rate equation is applicable only to a single extent of conversion and to the time region (Δt) related to this conversion. In other words, the isoconversional methods describe the kinetics of the process by using the multiple single rate (or single-step) kinetic equations, each of which is associated with a certain extent of conversion. With regard to this advantage, the isoconversional methods allow complex (i.e., multi-step) processes to be detected via a variation of the effective apparent activation energy ($E_{a\alpha}$) with conversion, α. Conversely, independence of $E_{a\alpha}$ on α is a sign of a single-step process.

The $E_{a\alpha}$–α correlation usually corresponds to the change of the reaction mechanisms; it may reflect relative contributions of parallel reaction channels to the overall reaction kinetics. In this article, the standard (Equation (12)) and Friedman (Equation (13)) isoconversional methods were used to analyze the mechanisms of the isothermal decomposition process of zinc leach residue.

Figure 7 shows the dependence of the effective apparent activation energy ($E_{a\alpha}$) in a function of the conversion fraction (α) evaluated by the standard (integral) and Friedman's (differential) isoconversional methods, for the decomposition process of the residue.

As shown in Figure 7, both the dependences have a progressively increasing character of the apparent activation energy (E_a), in the whole range of the considered conversion (α) values ($0.05 \leq \alpha \leq 0.95$). This behavior of E_a values with α is the characteristic for the processes involving parallel competing reactions (Vyazovkin 1996). Moreover, the E_a values calculated by using Friedman's isoconversional method are higher than the corresponding values of E_a calculated by using the standard (integral) isoconversional method. It was found that the calculated values of the apparent activation energies of competitive and independent reactions based on differential Friedman's isoconversional method ($E_{a\mathrm{dif}}$) and integral isoconversional method ($E_{a\mathrm{int}}$) give different values, calculated using Equations (13) and

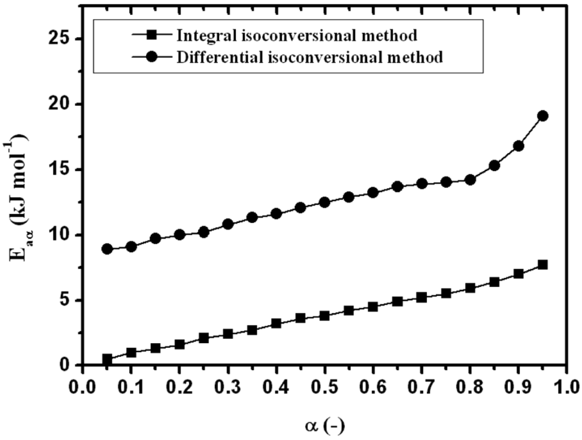

Figure 7. The dependence of the effective apparent activation energy ($E_{a\alpha}$) as a function of the conversion fraction (α) evaluated by the standard (integral) (symbol (■)) and the Friedman's (differential) (symbol (●)) isoconversional methods.

(12), respectively (Dowdy 1987). Therefore, two different values for $E_{a\mathrm{dif}}$ and $E_{a\mathrm{int}}$ for the narrower temperature range indicate the dependence $E_a = E_a(\alpha)$.

In the case of isothermal decomposition of zinc leach residue, the apparent activation energy varies in the range of 0.5–7.7–kJ mol^{-1}, with extremely low values of the preexponential factor. Based on the shape of dependence E_a on α (Figure 7), we may conclude that the investigated decomposition process takes place through the parallel competing reactions, which have different contributions to the overall process. However, it is possible to detect the total number of reactions present in the system, from the experimentally obtained density distribution function of the apparent activation energy ($f(E_a)$). The observed distribution can be obtained by the numerical differentiation of $\alpha = \alpha\ (E_a)$ dependence. The relationship between α versus E_a evaluated from the integral isoconversional method could be obtained by plotting the α values against the corresponding E_a values as shown in Figure 8.

When the curve was differentiated graphically by E_a, $f(E_a)$ distribution curve for isothermal decomposition process of zinc leach residue could be obtained as shown in Figure 9.

The peaks (designated as peaks I, II, III, and IV (Figure 9)) of the $f(E_a)$ distribution curve appear at the values of 1.3, 2.4, 3.7, and 5.2 kJ mol^{-1}, respectively, and the apparent activation energy spreads in the interval 0.5 kJ mol$^{-1} \leq \Delta E_a \leq 7.7$ kJ mol^{-1}. The widths of the observed peaks in the $f(E_a)$ distribution curve are as follows: 0.5, 0.6, 0.8, and 1.7 kJ mol^{-1} for I, II, III, and IV, respectively (Figure 9). The increase in the width of the peak is accompanied by an increase in the value of E_a. From the obtained results, we can *assume* that there are probably four reaction steps that occur in the following ranges of the degree of conversion (α) and the given values of E_a as: (a) the first step: 0.05 $\leq \alpha \leq 0.25$; $E_a = 0.5$–2.1 kJ mol^{-1}, (b) the second step: 0.25 $\leq \alpha \leq 0.40$; $E_a = 2.1$–3.2 kJ mol^{-1}, (c) the third step: 0.40 $\leq \alpha \leq 0.60$; $E_a = 3.2$–4.5 kJ mol^{-1}, and the fourth step: (d) 0.60 $\leq \alpha \leq 0.95$; $E_a = 4.5$–7.7 kJ mol^{-1}.

In accordance with Vyazovkin and Lesnikovich (1990), the increase of E_a values with increasing α is accompanied by a convex Arrhenius dependence, which

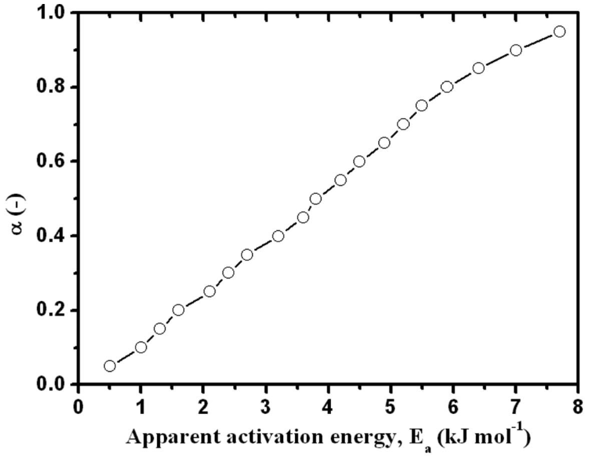

Figure 8. The α versus E_a relationship estimated from the integral isoconversional $E_a = E_a(\alpha)$ dependence.

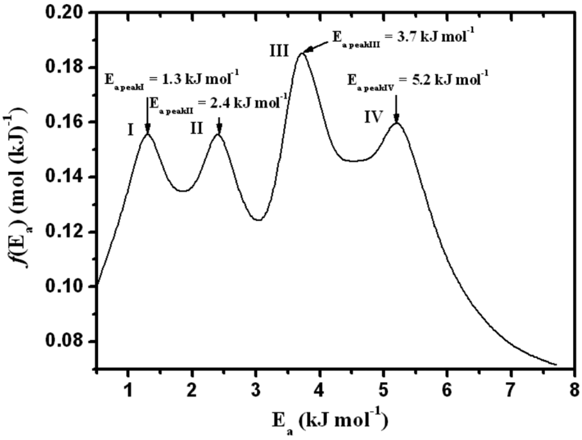

Figure 9. $f(E_a)$ density distribution curve estimated for the isothermal decomposition of zinc leach residue in an inert atmosphere.

is typical for a system of parallel competing reactions. The convex Arrhenius behavior is observed for the isothermal decomposition of zinc leach residue, as shown in Figure 10.

The convex ln$k$ versus $1/T$ dependence can occur due to the different thermal stability of the components of the investigated sample. This behavior is interpreted by the value of lower rate than that expected at high temperatures (in our case, it is probably for $T > 1000°C$), and this is very common in catalytic processes. This type of process is characterized by unusually very low preexponential factor (Table 3) and low values of the apparent activation energy. Namely, in the investigated isothermal decomposition of zinc leach residue, we have a complex autocatalytic process, which

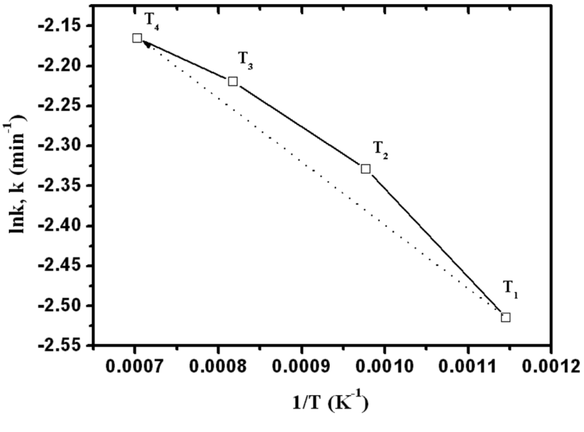

Figure 10. The Arrhenius feature as ln$k$ versus $1/T$ (T_1, T_2, T_3, and T_4 are the corresponding operating temperatures (lowest—T_1 and highest—T_4)), for the isothermal decomposition process of zinc leach residue (the dashed arrow in the direction from T_1 to T_4 is presented in order to better visibility of the deviations from the linear (nonconvex) dependence).

probably involves a system of competitive reactions, where each of these reactions is dominant in the different temperature regions, and the corresponding reactions can be presented in the following form:

$$\text{(Step 1)} \qquad PbSO_4 \rightarrow PbO + SO_2 + {}^1\!/_2\, O_2 \qquad (T < 1000°C) \qquad (23)$$

$$\text{(Step 2)} \qquad 3Fe_2O_3 \rightarrow 2Fe_3O_4 + {}^1\!/_2\, O_2 \qquad (T < 1000°C) \qquad (23a)$$

(reduction of Fe_2O_3 forming Fe_3O_4: the expected temperature range is $400°C < T < 650°C$)

$$\text{(Step 3)} \qquad Zn_2SiO_4 \rightarrow 2ZnO + SiO_2 \qquad (T < 1000°C) \qquad (23b)$$

(The oxides reduction continues with increasing temperature, and zinc oxide will be produced at a temperature of about 800°C (Saage and Hasche 2004) and at the temperature above 900°C, mainly zinc vapor is formed as one of the main products.)

$$\text{(Step 4)} \qquad 3ZnO \cdot Fe_2O_3 \rightarrow 3ZnO + 2Fe_3O_4 + {}^1\!/_2\, O_2 \qquad (T > 1000°C) \qquad (23c)$$

(The final production of zinc oxide (ZnO) is surely completed at the temperature of 1200°C.)

For the isothermal decomposition process of zinc leach residue, the convex curvature occurs as a result of "changes" of the set of atoms, i.e., at higher temperatures, the decomposition of complex compound into the noncomplex form of compounds occurred.

$ZnO \cdot Fe_2O_3$ (catalytic complex) is split at very high temperatures ($T > 1000°C$) in a noncomplex form as $ZnO + Fe_3O_4 + {}^1\!/_2\, O_2$. This can also be shown through the reaction in the following form:

$$\begin{aligned}[ZnFe_2O_4] : 3ZnO \times Fe_2O_3\ &\text{(Complex (catalytic))} \rightarrow \\ &3ZnO + 2Fe_3O_4 + {}^1\!/_2\, O_2\ \text{(High operating temperatures, } T \geq 1000°C\text{)}.\end{aligned} \qquad (24)$$

$ZnO \times Fe_2O_3$ is likely to be autocatalytically decomposed into ZnO and other chemical species, which significantly reduces the energy barrier for a given process. However, in the case of autocatalytic reaction, the reaction rate is strongly influenced by the concentration of the formed product. In the investigated decomposition process, the overall reaction rate strongly depends on the amount of obtained zinc oxide (ZnO). It should be noted that the molecular oxygen has to be evolved to complete the decomposition process, which is effectively implemented in the presence of oxide, such as Fe_2O_3 (Ju et al. 2011).

The considered decomposition process can be best described by the autocatalytic SB kinetic model, with the strong influence of operating temperatures on the reaction system. The complex mechanism probably involves a system of four parallel competitive reactions (Equations (23)–(23c)), where the autocatalytic behavior of the investigated process has the highest contribution at high operating temperatures.

CONCLUSION

The decomposition of zinc leach residue was processed under the isothermal conditions ($T = 600°\text{C}$, 750°C, 950°C, and 1150°C) in a tubular furnace, with a constant nitrogen gas flow rate. The characterization of the obtained product particles was conducted by XRD analyses.

Detailed kinetic analysis showed that the isothermal decomposition process of zinc leach residue can be described by the two-parameter autocatalytic SB kinetic model in the form of Equation (17), with the kinetic parameters: $E_a = 4.0\,\text{kJ mol}^{-1}$, $A = 0.1545\,\text{min}^{-1}$, $m = 0.199$, and $n = 0.591$. It was also found that the operating temperature has an influence on the values of the parameters m and n, and also on the values of the global reaction orders $(m + n)$. Also, it was established that the values of $m < 1$ means that the autocatalytic reaction has higher contribution on the overall reaction rate. It was found that the apparent activation energy values increase progressively with the degree of conversion, accompanied by the appearance of a convex Arrhenius dependence ($\ln k$ versus $1/T$). This behavior is characteristic for a system of parallel competitive reactions, where the autocatalytic behavior of the considered process has the highest contribution at high operating temperatures.

It was concluded that the investigated isothermal decomposition process is characterized by unusually very low preexponential factor and low values of the apparent activation energy. Based on the derived density distribution function of E_a values, it was concluded that the isothermal decomposition process probably occurs through four reaction steps, where each step is characterized by one parallel reaction.

ACKNOWLEDGMENTS

The authors would like to thank Deutsche Forschungsgemeinschaft DFG in Bonn for financial support of the project FR 1713/13-1: Zn-recovery from steel making dusts—Kinetics and mechanism of thermal zinc–ferrite phase decomposition (Srećko Stopić, Aybars Güven, and Bernd Friedrich).

The authors would also like to thank the Ministry of Science and Environmental Protection of Serbia under the Project 172015 (Bojan Janković).

REFERENCES

Bamford, C. H. and Tipper, C. H. F., 1980, *Comprehensive Chemical Kinetics: Reactions in the Solid State*, Vol. 22, 1st ed., Amsterdam: Elsevier, pp. 30–70.

Brown, M. E. and Galwey, A. K., 1989, "Arrhenius parameters for solid-state reactions from isothermal rate-time curves." *Analytical Chemistry*, 61, pp. 1136–1139.

Burnham, A. K. and Braun, R. L., 1999, "Global kinetic analysis of complex materials." *Energy and Fuels*, 13, pp. 1–22.

Dowdy, D. R., 1987, "Meaningful activation energies for complex systems II. Evaluation of the Friedman method when applied to multiple reactions, and comparison with the

Ozawa-Flynn-Wall method.” *Journal of Thermal Analysis and Calorimetry*, 32, pp. 1177–1187.

Friedman, H. L., 1964, “Kinetics of thermal degradation of char-forming plastics from thermogravimetry-application to a phenolic resin.” *Journal of Polymer Science Part C*, 6, pp. 183–195.

Galwey, A. K. and Brown, M. E., 1999, *Thermal Decomposition of Ionic Solids*, 1st Ed., Amsterdam: Elsevier, pp. 75–110.

Havlik, T., Turzakova, M., Stopić, S., and Friedrich, B., 2007, “Atmospheric leaching of EAF dust with diluted sulphuric acid.” *Hydrometallurgy*, 77, pp. 41–50.

Ju, S., Zhang, Y., Zhang, Y., Xue, P., and Wang, Y., 2011, “Clean hydrometallurgical route to recover zinc, silver, lead, copper, cadmium and iron from hazardous jarosite residues produced during zinc hydrometallurgy.” *Journal of Hazardous Materials*, 192, pp. 554–558.

Kaneko, H., Kodama, T., Gokon, N., Tamura, Y., Lovegrove, K., and Luzzi, A., 2004, “Decomposition of Zn-ferrite for O_2 generation by concentrated solar radiation.” *Solar Energy*, 76(1–3), pp. 317–322.

Málek, J., 1992, “The kinetic analysis of non-isothermal data.” *Thermochimica Acta*, 200, pp. 257–269.

Málek, J. and Smrčka, V., 1991, “The kinetic analysis of the crystallization processes in glasses.” *Thermochimica Acta*, 186(1), pp. 153–163.

Radović, N., Amberović, Z., and Panias, D., 2009, “Cleaner metallurgical industry in Serbia: A road to the sustainable development.” *Chemical Industry & Chemical Engineering Quarterly*, 15(1), pp. 1–4.

Roşu, D., Caşcaval, C. N., Mustaţă, F., and Ciobanu, C., 2002, “Cure kinetics of epoxy resins studied by non-isothermal DSC data.” *Thermochimica Acta*, 383, pp. 119–127.

Saage, E. and Hasche, U., 2004, “Optimisation of the Waelz process at the B.U.S. Zinkrecycling Freiberg GmbH.” *World of Metallurgy – ERZMETALL*, 57, pp. 138–142.

Šesták, J. and Berggren, G., 1971, “Study of the kinetics of the mechanism of solid-state reactions at increasing temperatures.” *Thermochimica Acta*, 3, pp. 1–12.

Stopić, S. and Friedrich, B., 2009, “Kinetics and mechanism of thermal zinc-ferrite phase decomposition.” *Proceeding of EMC 2009*, Innsbruck, Austria, June 28–July 1, 2009, pp. 1167–1181.

Štrbac, N., Mihajlović, I., Andrić, V., Živkovic, Ž., and Rosić, A., 2011, “Kinetic investigations of two processes for zinc recovery from zinc plant residue.” *Canadian Metallurgical Quarterly*, 50, pp. 28–34.

Turmanova, S. Ch., Genieva, S. D., Dimitrova, A. S., and Vlaev, L. T., 2008, “Non-isothermal degradation kinetics of filled with rise husk ash polypropene composites.” *eXPRESS Polymer Letters*, 2, pp. 133–146.

Vyazovkin, S., 1996, “A unified approach to kinetic processing of nonisothermal data.” *International Journal of Chemical Kinetics*, 28, pp. 95–101.

Vyazovkin, S., 2000, “Computational aspects of kinetic analysis. Part C. The ICTAC kinetics project—the light at the end of the tunnel?” *Thermochimica Acta*, 355, pp. 155–163.

Vyazovkin, S. and Wight, C. A., 1999, “Model-free and model-fitting approaches to kinetic analysis of isothermal and nonisothermal data.” *Thermochimica Acta*, 340–341, pp. 53–68.

Vyazovkin, S. V. and Lesnikovich, A. I., 1990, “An approach to the solution of the inverse kinetic problem in the case of complex processes: Part 1. Methods employing a series of thermoanalytical curves.” *Thermochimica Acta*, 165, pp. 273–280.